

Journal of Biomedical Optics

SPIEDigitalLibrary.org/jbo

Qualitative investigation of fresh human scalp hair with full-field optical coherence tomography

Woo June Choi
Long-Quan Pi
Gihyeon Min
Won-Soo Lee
Byeong Ha Lee

Qualitative investigation of fresh human scalp hair with full-field optical coherence tomography

Woo June Choi,^a Long-Quan Pi,^b Gihyeon Min,^a Won-Soo Lee,^b and Byeong Ha Lee^a

^aSchool of Information and Communications, Gwangju Institute of Science and Technology (GIST), 261 Cheomdan-gwagiro, Buk-gu, Gwangju, 500-712, Republic of Korea

^bDepartment of Dermatology and Institute of Hair and Cosmetic Medicine, Yonsei University, Wonju College of Medicine, Wonju, Republic of Korea

Abstract. We have investigated depth-resolved cellular structures of unmodified fresh human scalp hairs with ultrahigh-resolution full-field optical coherence tomography (FF-OCT). The Linnik-type white light interference microscope has been home-implemented to observe the micro-internal layers of human hairs in their natural environment. In hair shafts, FF-OCT has qualitatively revealed the cellular hair compartments of cuticle and cortex layers involved in keratin filaments and melanin granules. No significant difference between black and white hair shafts was observed except for absence of only the melanin granules in the white hair, reflecting that the density of the melanin granules directly affects the hair color. Anatomical description of plucked hair bulbs was also obtained with the FF-OCT in three-dimensions. We expect this approach will be useful for evaluating cellular alteration of natural hairs on cosmetic assessment or diagnosis of hair diseases. © 2012 Society of Photo-Optical Instrumentation Engineers (SPIE). [DOI: 10.1117/1.JBO.17.3.036010]

Keywords: fresh human scalp hair; cuticle and cortex; melanin granule; hair bulb; full-field optical coherence tomography; label-free three-dimensional imaging.

Paper 11496 received Sep. 9, 2011; revised manuscript received Dec. 14, 2011; accepted for publication Jan. 4, 2012; published online Apr. 4, 2012.

1 Introduction

Human hair is a keratinous biological fiber with well-characterized cellular composites. For a number of decades, hair fiber has been the subject of intense scientific research in dermatology and cosmetology.¹⁻³ In particular, structural characterization of hair has been of special interest because the morphological features of hair have provided important biophysical clues for early diagnosis of skin disease⁴ and breast cancer,⁵ cosmetic assessment,⁶ and forensic examination.⁷ Classically, ultrastructural observation of human hair has been widely performed by using scanning electron microscopy (SEM) and transmission electron microscopy (TEM).^{8,9} Although the microscopic assays are efficient and well-established, the sample preparation is time-consuming and laborious. It even may deform the intrinsic hair structures during cutting, vacuum evaporating, gold coating, and chemical treatments. Atomic force microscopy (AFM) and confocal laser scanning microscopy (CLSM) have emerged as alternatives for noninvasive examination of the hair structure.¹⁰⁻¹² These techniques, compared with the electron microscopy techniques, offer three-dimensional (3-D) cellular images of the hairs with minimal sample preparation. However, AFM is only available for hair surface topography,¹⁰ and CLSM needs additional fluorescence marking of the hair layers for internal exploration.^{6,11,12} Further, in confocal imaging, some fluorescence signals in the regions away from the focal point might pass through the pinhole, thereby increasing emission background. Phototoxic effect of fluorophore with the laser illumination also may hamper hair cell viability. Cross-polarized CLSM (CP-CLSM), a variant of the confocal imaging regime, has provided contrast-enhanced

hair imaging using polarization dependence of birefringent hair structures without aid of any chemical labeling.^{13,14} However, use of the technique is rather specialized in fully keratinized hair structures like cortex. Multiphoton microscopy such as two-photon excitation microscopy (TPEM) or second harmonic generation microscopy (SHM) has been employed for internal investigation of the hair.^{15,16} Its nonlinear excitation using a near-infrared light allowed high-resolution fluorescence imaging of the hair with long penetration depth and a small risk of photo damage. Recent effort to image the healthy state of hair without any processing or treatment has been conducted by using hard x-ray microscopy.¹⁷ The submicron spatially resolved phase contrast image showed the internal details of the hair shaft. But the long radiation of x-ray (~60 s) onto the hair also might induce morphological change to the hair,¹⁸ and its projection view is not suitable to observe hair structures in depth.

Optical coherence tomography (OCT) is noninvasive optical biopsy for obtaining 3-D tissue morphology using low coherence-gated detection of the light scattered from a turbid specimen, where exogenous contrast agents and special sample preparation are not involved.¹⁹ This modality has been widely exploited for biological,²⁰ medical,²¹ and material²² applications. Recently, OCT has been used for hair imaging, proposing potential for characterization of natural hair interior.²³⁻²⁵ But the previous OCT works have failed to reveal the complex internal micro-architectures of the hair due to their poor spatial resolution (a few tens of micrometers). Hence substantial cellular morphology of the natural hair still remains unexplored.

In this article, we report prospective approach to hair characterization using subcellular resolution OCT and present the tangible findings in the hair morphology. Ultrahigh-resolution full-field OCT (FF-OCT),²⁶⁻³¹ an expansion of OCT technology,

Address all correspondence to: Byeong Ha Lee, School of Information and Communications, Gwangju Institute of Science and Technology (GIST), 261 Cheomdan-gwagiro, Buk-gu, Gwangju, 500-712, Republic of Korea. Tel: 82-62-715-2234; Fax: 82-62-715-2204; E-mail: leebh@gist.ac.kr

is employed to achieve cellular *en-face* tomographic images of hairs in a spatial resolution (axial and lateral) down to $\sim 1 \mu\text{m}$, provided by a thermal light source and high NA (numerical aperture) objectives. Overlapping the short coherence gate ($\sim 1 \mu\text{m}$) of FF-OCT to the focal plane enables effective rejection of image-clouding bearing multiple-scattered light in turbid media, providing label-free high-resolution tomographic images. The potential of FF-OCT for subcellular level imaging in various fields has been demonstrated.^{32,33} With the FF-OCT, in this study we capture a series of *en-face* tomographic images of cut hair shafts and plucked hair bulbs with a depth step of $0.5 \mu\text{m}$. In particular, we qualitatively reveal that density of melanin granule in the cortex region would be a dominant factor to determine hair color intensity. To our best knowledge, we first demonstrate the 3-D histological description of hair cells in natural state.

2 Material and Methods

A home-implemented FF-OCT system was utilized for natural hair observation (Fig. 1). The OCT microscope consisted of a Linnik-type white light interferometer similar to the previous works.^{29,31} A nonpolarized 100-W halogen bulb was used as a light source with a standard Köhler illumination setup, and a silicon-based charge-coupled device (CCD) camera was used as an image sensor. The effective source spectrum of the system was Gaussian-like and centered at 650 nm with FWHM of 220 nm; it gives a coherence length of $1.9 \mu\text{m}$ corresponding with an axial resolution of $0.8 \mu\text{m}$ in water. A pair of water immersion objectives ($\times 100$, NA 1.0 in water) provided a theoretically high lateral resolution of about $0.4 \mu\text{m}$. The lights back-reflected from both arms and making interference with each other were projected and pixilated by the CCD chip (1024×1024 pixels, 12-bit, 20 fps). Optical path length of the reference arm was modulated with a piezo-actuator (PZT), leading relative phase change to the sample arm.

From a series of CCD images, subsequently captured during one cycle of the PZT modulation, a background-free *en-face*

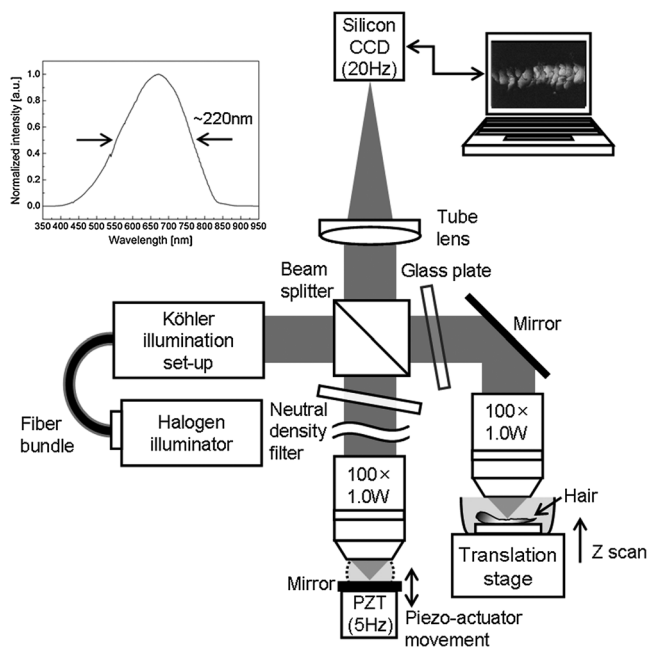


Fig. 1 Schematic of the FF-OCT system based on a Linnik-type white light interferometer. Inset shows the effective spectrum of the system.

image of a sample could be obtained;³¹ a 2-D cross-sectional XY plane image at a certain depth across the sample. The system hardware and processing were computer-controlled, which allowed quasi-real time display of the OCT images at a speed of five frames/s. For 3-D OCT imaging, the sample was axially scanned using a motorized translation stage with a step of $0.5 \mu\text{m}$. The z-stacked OCT data set was volume-rendered with commercial rendering software (Amira 5.3.2, Visage Imaging Inc., San Diego, CA).

A total of 20 human hair samples (12 black, four dark brown, and four white) were collected from the vertex regions of scalps, which were plucked or cut at the proximal root from 16 Korean volunteers ages 24 to 42 years. The volunteers had never been treated with any chemical reactions, such as coloring or permanent waving. In the plucked hairs, the hair bulbs in the anagen phase were selected under a dissection microscope. The hair strips were rinsed thoroughly for 1 min with 99.9% ethyl alcohol to remove dusts or hand oils followed by air-drying at room temperature for 5 min. The cleaned hair body was lightly pressed and attached to a container with double-sided tape. The container was filled with pure water and placed on the OCT microscope sample stage. OCT imaging was performed in two different regions of the hair; the proximal root end of the cut hair and the lower part (i.e., hair bulb) of the plucked hair follicle, respectively. The acquisition time for each *en-face* tomographic image (five images were averaged) was 1 sec.

3 Experimental Results

3.1 Hair Shaft Imaging

Several hair shafts with different colors were imaged with the FF-OCT system. Figure 2 shows *en-face* OCT images, taken at different depths, of a black hair shaft (male, age 29) near to the proximal root end of the hair. We can see the cuticle as the outmost portion of the hair shaft is composed of many overlapping scale-like cells leaned toward the distal end of the hair shaft in Fig. 2(a). Figure 2(b) is the tomogram taken at a depth of $4 \mu\text{m}$ below the cuticle surface, showing that the cortex layer contains keratin filaments closely packed with longitudinal orientation and melanin granules embedded into the keratinous structures. Inset of Fig. 2(b) indicates that these melanin granules are oval or ellipsoidal with $\sim 1 \mu\text{m}$ long size (arrows), showing typical characteristics of eumelanins.³⁴ In Fig. 2(c) and Fig. 2(d), aggregation of the melanin granules is observed inside the cortical region. It is especially interesting to see that several rows of spindle-shaped air pockets called the cortical fusi (asterisks) are interspersed parallel to the hair shaft and seem to be tightly packed by mass of the melanin granules in the cortex.

Figure 3 shows FF-OCT images of a dark brown hair shaft (male, age 30), taken at the hair surface (a) and $4 \mu\text{m}$ (b), $9 \mu\text{m}$ (c), $12 \mu\text{m}$ (d) below the surface, respectively. In Figs. 3(c) and 3(d), we can see that amount of the melanin granules in the dark brown hair shaft is much less than that of the black hair shaft shown in Figs. 2(c) and 2(d). Furthermore, the melanin granules are widely dispersed over the cortex and a few of cortical fusi (asterisks) are clearly visible in the cortex.

In contrast with the black hair shaft and the dark brown hair shaft, FF-OCT images of a white hair shaft (male, age 42) reveal absence of the melanin granules within the cortex as shown in Fig. 4. This finding clarifies many previous claims that density

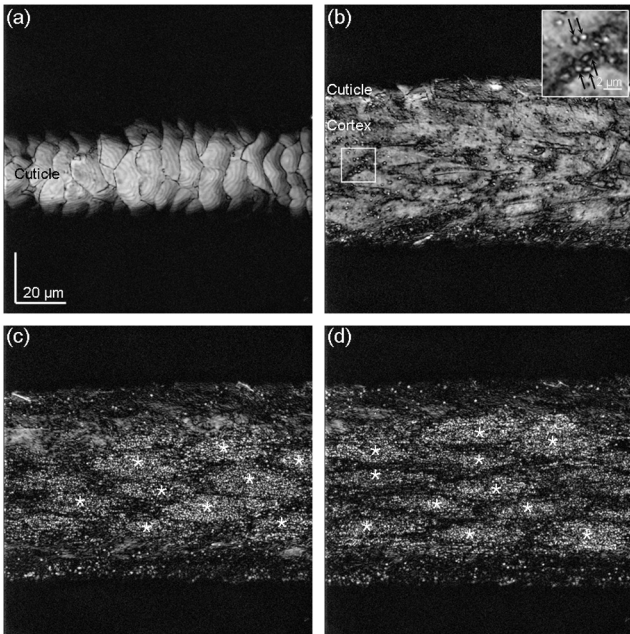


Fig. 2 *En-face* (XY) OCT images of a human scalp black hair shaft taken at the hair surface (a) and at depths of 4 μm (b), 6 μm (c), and 7 μm (d) below the surface. At depth of 4 μm , keratin matrix and melanin granules are visible in the cortex (b). Inset is an enlarged view of the region of interest (ROI), saying typical eumelanin (arrows). In (c) and (d), aggregation of the melanin granules is evident. Note that spindle-shaped cortical fusi appear to be sheathed by many of the granules (asterisks).

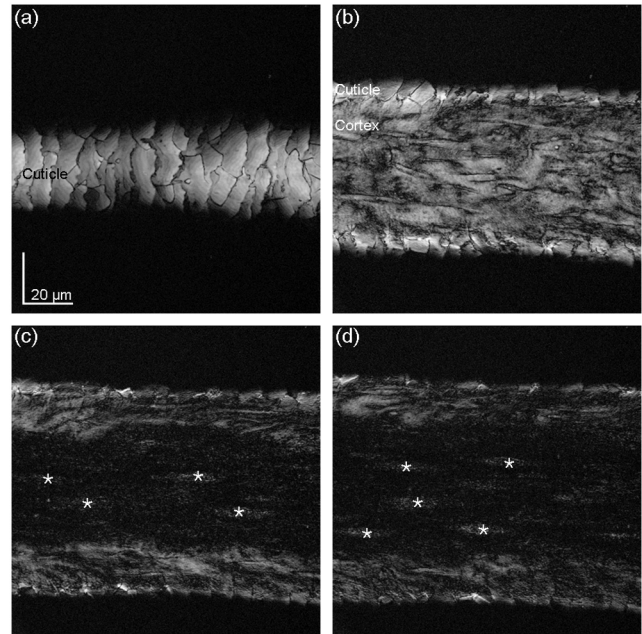


Fig. 4 *En-face* (XY) OCT images of a human scalp white hair shaft taken at the hair surface (a) and at depths of 4 μm (b), 6 μm (c), and 7 μm (d) below the surface. There is no significant difference in structure from the black hair except lack of the melanin granules in the cortex. Cortical fusi appears at asterisks in (c) and (d).

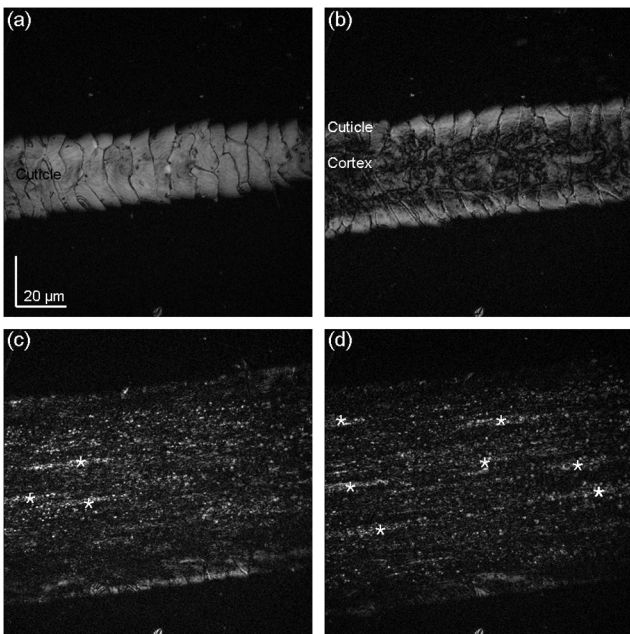


Fig. 3 *En-face* (XY) OCT images of a human scalp dark brown hair shaft taken at the hair surface (a) and at depths of 4 μm (b), 9 μm (c), and 12 μm (d) below the surface. Density of the melanin granule in the cortex is much less than that of the black hair shaft. A few of cortical fusi (asterisks) are visible in (c) and (d).

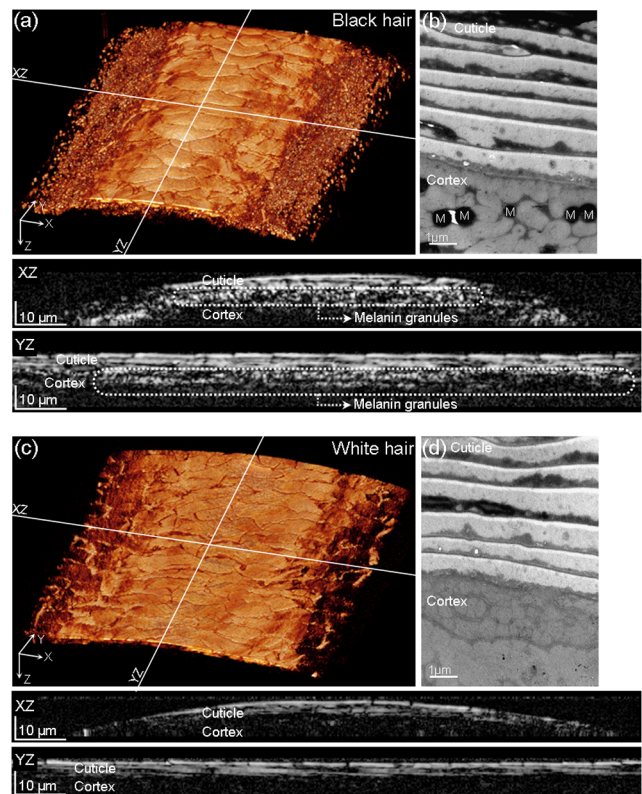


Fig. 5 Three-dimensional OCT images of human scalp black (a) and white (c) hair shafts, and representative cross-sectional (XZ) transmission electron microscopy (TEM) images ($\times 20,000$) of the same type of black (b) and white (d) hair shafts. Distinct difference in density of the melanin granules between them is confirmed with the cross-sectional images (XZ and YZ sections) taken along the white lines of (a) and (c). Dotted circles indicate cluster of the melanin granules. The melanin granules (M) are evident in the black hair cortex (b).

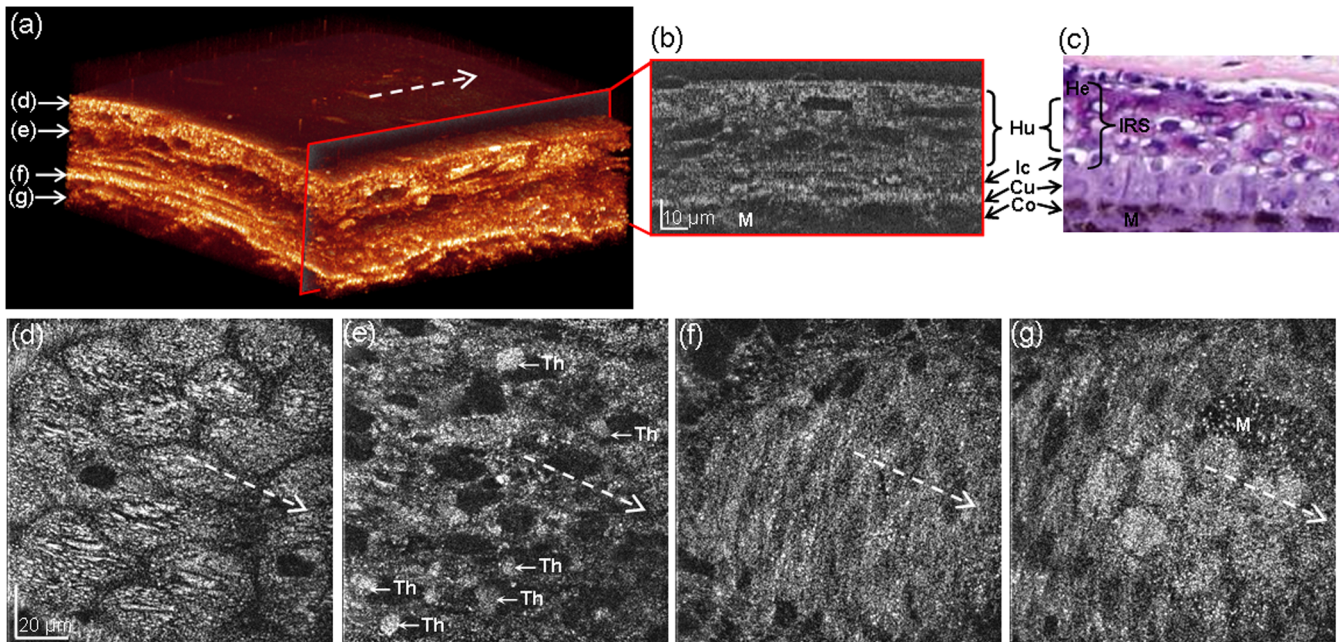


Fig. 6 Volume rendering of OCT image [$120\ \mu\text{m}$ (X) \times $120\ \mu\text{m}$ (Y) \times $54\ \mu\text{m}$ (Z)] of a human black hair bulb (a) and some of *en-face* images taken at depths of $10.5\ \mu\text{m}$ (d), $18.5\ \mu\text{m}$ (e), $28.5\ \mu\text{m}$ (f), and $32\ \mu\text{m}$ (g) below the surface. Each snapshot reveals individual cellular compartments inside the hair bulb; (d) and (e) Huxley layers of inner root sheath (IRS), (f) hair cuticle, and (g) hair cortex. The cross-sectional view (red box) of the 3-D rendering of the hair bulb (b) is well correlated with the representative H&E stained histology of the same type of hair bulb (c). Dotted arrows indicate the direction to the distal end of the hair. IRS: inner root sheath, He: Henle layer, Hu: Huxley layer, Ic: IRS cuticle, Cu: hair cuticle, Co: hair cortex, Th: trichohyalin granule, and M: melanosome.

of the melanin granules in the cortex is responsible for hair pigmentation.^{35–37} We also obtained the same results with the hairs of several subjects.

Figure 5(a) and 5(c) show 3-D OCT images of a black hair shaft and a white hair shaft, respectively, obtained from a stack of such *en-face* tomograms. The 3-D reconstruction allows visualization of the perspective hair shafts, which makes it comprehensible at a glance to identify difference of density of the melanin granules between both hair fibers. This structural difference is significantly shown by comparing them in the vertical cross-sectional views [XZ and YZ sections along the white lines in Fig. 5(a) and 5(c)] of the 3D-OCT images. Note that XZ OCT images are well correlated with representative cross-sectional (XZ) TEM images of the same type of the hair shafts [Fig. 5(b) and 5(d)].

3.2 Plucked Hair Bulb Imaging

Figure 6 shows a 3-D rendering image of a plucked black hair bulb (female, age 28) (a), reconstructed by stacking 108 *en-face* OCT tomograms and some of *en-face* snapshot images taken at different depths (d to g). From Fig. 6(d), we estimate that the single layer of the cornified horny cells would be some portion of the Huxley layer at the second innermost layer of inner root sheath (IRS) in the hair follicle. In general, the IRS features three distinct epithelial layers, namely the Henle layer, Huxley layer, IRS cuticle (from outmost and innermost), and the Huxley layer has one or two layers of horny, nucleated cells.⁸ Figure 6(e) shows the immediately following the other Huxley layer, where presumptive trichohyalin granules (Th) are developing at the level of the keratinized hair. Figure 6(f) is the *en-face* cut made at a $28.5\text{-}\mu\text{m}$ depth, showing single-layered hair cuticle cells near to the IRS. It is easily recognizable that the hair cortex

located just below the hair cuticle has hexagon-like cells and numerous melanosomes (M) as shown in Fig. 6(g). Figure 6(b) is a XZ cross-section of the 3-D OCT hair bulb image [indicated with a red box in Fig. 6(a)], which is well correlated with a representative H&E stained histology section of the same type of hair bulb in Fig. 6(c).

4 Conclusion and Discussion

In summary, full-field optical coherence tomography (FF-OCT) has been demonstrated for structural investigation of human scalp hairs in native environment. Compared with conventional systems for hair imaging, FF-OCT exhibited anatomical description of even hair cells while preserving intact hair state. Such histology-like appearances confirmed that color of hair primarily depends on aggregation of melanin granules in the cortical region of the hair, which agreed with TEM results. Moreover, this technique allowed the observation of fine cell structures of hair bulb in three dimensions. Though qualitative interpretation of the hair fibers was highlighted in this study, it would be applicable to improve our understanding of living hair morphology even at cellular level, which has been fairly challenging with the conventional techniques. This approach is very useful for monitoring the progressive change of hair structure in four dimensions (3-D space over time). Thus we can find the potential applications for dynamic hair researches ranging from cosmetic evaluation to diagnosis and treatment effect of hair disorder. For example, photo-aging of human hair induces change in hair color, which is understood to be involved in oxidative attack on melanosome by exposure to UV radiation like sunlight.³⁸ Depth-resolved cellular imaging of FF-OCT allows identification of melanin granules in the cortical region of a hair shaft, which might be useful for investigating the hair photo-aging effect by quantitatively evaluating the temporal

change in density of the melanin granules in the cortex. Moreover, since the trichohyalin granule in the IRS of a hair follicle is known as one of potential major auto-antigen in human alopecia areata,³⁹ FF-OCT evaluation of trichohyalin population in the hair follicle would be informative for early diagnoses of the hair-loss disease.

Despite these benefits, the penetration depth in hair imaging was limited beyond tens of micrometers because the refractive index (RI) of the hair ($n = 1.56 \sim 1.59$) is rather big.²³ The big RI, relative to its surroundings, induces a kind of optical aberration when imaging a sample in a depth; segregation of the focusing plane from the coherence gating plane happens.⁴⁰ Use of an index matching oil similar to the hair RI as an immersion medium is a simple option for reducing this dispersion issue, but it requires specific oil-immersion objectives in both arms of the interferometer. Recently, Min et al. has proposed a numerical correction method to rejuvenate the degraded OCT images.⁴¹ The method uses the phase-shifting digital holographic technique⁴² based on the Fresnel-Kirchhoff diffraction theory, which numerically relocates the defocused sample at the virtual focal plane. Ideally, a fully focused OCT image can be constructed regardless of the degree of optical distortion along the depth of the sample. Adoption of this correction technique to the FF-OCT system would be helpful to improve the imaging depth without appreciable signal degradation. Of course, using the birefringence of the cortex might be helpful for enhancing the visibility of the image, which is under investigation.⁴³

Our standard FF-OCT setup, which uses a bulk interference microscope, is not easily accessible for imaging the hairs on a human scalp because of its rigid configuration. However, *in vivo* imaging of hairs is of great importance for clinical applications in practice. Recently, Latrive et al. has opened the possibility of *in vivo* FF-OCT imaging using a compact needle-like probe and two coupled interferometers.⁴⁴ Therefore, we expect that the FF-OCT will be readily available in the near future to observe the hair structures *in vivo* for clinical and cosmetic purposes.

Acknowledgments

This study was supported by a grant of the Korean Health Technology R&D project, Ministry for Health, Welfare & Family Affairs, Republic of Korea (No. A100490), and the Ministry of Knowledge and Economy of Korea through the Ultrashort Quantum Beam Facility Program.

References

1. T. Soma et al., "Analysis of apoptotic cell death in human hair follicles *in vivo* and *in vitro*," *J. Invest. Dermatol.* **111**(6), 948–954 (1998).
2. H. K. Bustard and R. W. Smith, "Investigation into the scattering of light by human hair," *Appl. Opt.* **30**(24), 3485–3491 (1991).
3. M. S. C. Birbeck, E. H. Mercer, and N. A. Barnicot, "The structure and formation of pigment granules in human hair," *Exp. Cell Res.* **10**(2), 505–514 (1956).
4. K. S. Kim et al., "Investigation of hair shaft in seborrheic dermatitis using atomic force microscopy," *Skin Res. Technol.* **17**(3), 288–294 (2011).
5. G. L. Corino and P. W. French, "Diagnosis of breast cancer by x-ray diffraction of hair," *Int. J. Cancer* **122**(4), 847–856 (2008).
6. C. Hadjur et al., "Cosmetic assessment of the human hair by confocal microscopy," *Scanning* **24**(2), 59–64 (2002).
7. R. E. Bisbing and M. F. Wolner, "Microscopical discrimination of twins' head hair," *J. Forensic. Sci.* **29**(3), 780–786 (1984).

8. G. E. Rogers, "Some aspects of the structure of the inner root sheath of hair follicles revealed by light and electron microscopy," *Exp. Cell Res.* **14**(2), 378–387 (1958).
9. R. C. C. Wagner et al., "Electron microscopic observations of human hair medulla," *J. Microsc.* **226**(Pt. 1), 54–63 (2007).
10. B. Bhushan and N. Chen, "AFM studies of environmental effects on nanomechanical properties and cellular structure of human hair," *Ultramicroscopy* **106**(8–9), 755–764 (2006).
11. P. Corcuff et al., "3-D reconstruction of human hair by confocal microscopy," *J. Soc. Cosmet. Chem.* **44**, 1–12 (1993).
12. J. M. Lagarde et al., "Confocal microscopy of hair," *Cell Biol. Toxicol.* **10**(5–6), 301–304 (1994).
13. A. Kharin et al., "Optical properties of the medullar and the cortex of human scalp hair," *J. Biomed. Opt.* **14**(2), 024035 (2009).
14. B. Varghese et al., "Contrast improvement in scattered light confocal imaging of skin birefringent structures by depolarization detection," *J. Biophotonics* **4**(11–12), 850–858 (2011).
15. J. G. Lyubovitsky et al., "In situ multiphoton optical tomography of hair follicles in mice," *J. Biomed. Opt.* **12**(4), 044003 (2007).
16. A. Ehlers et al., "Multiphoton fluorescence lifetime imaging of human hair," *Microsc. Res. Techniq.* **70**(2), 154–161 (2007).
17. H. S. Youn and S.-W. Jung, "Observations of a human hair shaft with an x-ray microscope," *Phys. Med. Biol.* **50**(22), 5417–5420 (2005).
18. M. L. Griem and K. Ranniger, "Modification of the radiation effect on hair roots of the mouse by actinomycin," *Radiat. Res.* **17**(1), 92–100 (1962).
19. J. G. Fujimoto, "Optical coherence tomography for ultrahigh resolution *in vivo* imaging," *Nat. Biotechnol.* **21**(11), 1361–1367 (2003).
20. W. Tan et al., "Optical coherence tomography of cell dynamics in three-dimensional tissue models," *Opt. Express* **14**(16), 7159–7171 (2006).
21. A. M. Zysk et al., "Optical coherence tomography: a review of clinical development from bench to bedside," *J. Biomed. Opt.* **12**(5), 051403 (2007).
22. S. K. Debnath et al., "Spectrally resolved phase-shifting interference microscopy: technique based on optical coherence tomography for profiling a transparent film on a patterned substrate," *Appl. Opt.* **49**(34), 6624–6629 (2010).
23. X. J. Wang et al., "Characterization of human scalp hairs by optical low-coherence reflectometry," *Opt. Lett.* **20**(6), 524–526 (1995).
24. M. V. R. Velasco et al., "Prospective ultramorphological characterization of human hair by optical coherence tomography," *Skin Res. Technol.* **15**(4), 440–443 (2009).
25. N. G. Bartels et al., "Hair shaft abnormalities in alopecia areata evaluated by optical coherence tomography," *Skin Res. Technol.* **17**(2), 201–205 (2011).
26. A. Dubois et al., "High-resolution full-field optical coherence tomography with a Linnik microscope," *Appl. Opt.* **41**(4), 805–812 (2002).
27. L. Vabre, A. Dubois, and A. C. Boccara, "Thermal-light full-field optical coherence tomography," *Opt. Lett.* **27**(7), 530–532 (2002).
28. B. Laude et al., "Full-field optical coherence tomography with thermal light," *Appl. Opt.* **41**(31), 6637–6645 (2002).
29. A. Dubois et al., "Three-dimensional cellular-level imaging using full-field optical coherence tomography," *Phys. Med. Biol.* **49**(7), 1227–1234 (2004).
30. W. Y. Oh et al., "Spectrally modulated full-field optical coherence microscopy for ultrahigh-resolution endoscopic imaging," *Opt. Express* **14**(19), 8675–8684 (2006).
31. A. Dubois et al., "Ultrahigh-resolution full-field optical coherence tomography," *Appl. Opt.* **43**(14), 2874–2883 (2004).
32. W. J. Choi et al., "Full-field optical coherence microscopy for identifying live cancer cells by quantitative measurement of refractive index distribution," *Opt. Express* **18**(22), 23285–23295 (2010).
33. W. J. Choi et al., "Characterization of wet pad surface in chemical mechanical polishing (CMP) process with full-field optical coherence tomography (FF-OCT)," *Opt. Express* **19**(14), 13343–13350 (2011).
34. Y. Liu et al., "Comparison of structural and chemical properties of black and red human hair melanosomes," *Photochem. Photobiol.* **81**(1), 135–144 (2005).
35. D. G. Vernall, "A study of the density of pigment granules in hair from four races of men," *Amer. J. Phys. Anthropol.* **21**(4), 489–496 (1963).

36. J. Steffensen, "Human hair pigment and hair colour," *J. Roy. Anthropol. Inst. G.* **82**(2), 524–526 (1952).
37. T. Takizawa et al., "Ultrastructure of human scalp hair shafts as revealed by freeze-substitution fixation," *Anat. Rec.* **251**(3), 406–413 (1998).
38. W.-S. Lee, "Photo-aggravation of hair aging," *Int. J. Trichology* **1**(2), 94–99 (2009).
39. S. Inui, T. Nakajima, and S. Itami, "Coudability hairs: a revisited sign of alopecia areata assessed by trichoscopy," *Clin. Exp. Dermatol.* **35**(4), 361–365 (2010).
40. S. Labiau et al., "Defocus test and defocus correction in full-field optical coherence tomography," *Opt. Lett.* **34**(10), 1576–1578 (2009).
41. G. Min et al., "Numerical correction of distorted images in full-field optical coherence tomography," *Meas. Sci. Technol.* **23**(3), 035403 (2012).
42. M. K. Kim, "Applications of digital holography in biomedical microscopy," *J. Opt. Soc. Korea* **14**(2), 77–89 (2010).
43. G. Moneron, A. C. Boccara, and A. Dubois, "Polarization-sensitive full-field optical coherence tomography," *Opt. Lett.* **32**(14), 2058–2060 (2007).
44. A. Latrive and A. C. Boccara, "In vivo and in situ cellular imaging full-field optical coherence tomography with a rigid endoscopic probe," *Biomed. Opt. Express* **2**(10), 2897–2904 (2011).